Physiol Genomics 42: 384–396, 2010.
First published May 11, 2010; doi:10.1152/physiolgenomics.00117.2009.

Highly conserved transcriptional responses to mechanical ventilation of the lung

Kenneth S. Kompass,[1] Gaetan Deslee,[2] Carla Moore,[2] Donald McCurnin,[3] and Richard A. Pierce[2]

[1]*Department of Ophthalmology and Visual Sciences and* [2]*Division of Pulmonary and Critical Care Medicine, Department of Internal Medicine, Washington University School of Medicine, St. Louis, Missouri; and* [3]*Department of Pediatrics, University of Texas Health Science Center, San Antonio, Texas*

Submitted 17 July 2009; accepted in final form 5 May 2010

Kompass KS, Deslee G, Moore C, McCurnin D, Pierce RA. Highly conserved transcriptional responses to mechanical ventilation of the lung. *Physiol Genomics* 42: 384–396, 2010. First published May 11, 2010; doi:10.1152/physiolgenomics.00117.2009.—Cross-species analysis of microarray data has shown improved discriminating power between healthy and diseased states. Computational approaches have proven effective in deciphering the complexity of human disease by identifying upstream regulatory elements and the transcription factors that interact with them. Here we used both methods to identify highly conserved transcriptional responses during mechanical ventilation, an important therapeutic treatment that has injurious side effects. We generated control and ventilated whole lung samples from the premature baboon model of bronchopulmonary dysplasia (BPD), processed them for microarray, and combined them with existing whole lung oligonucleotide microarray data from 85 additional control samples from mouse, rat, and human and 19 additional ventilated samples from mouse and rat. Of the 2,531 orthologs shared by all 114 samples, 60 were modulated by mechanical ventilation [false discovery rate (FDR)-adjusted q value (q_{FDR}) = 0.005, ANOVA]. These included transcripts encoding the transcription factors ATF3 and FOS. Because of compelling known roles for these transcription factors, we used computational methods to predict their targets in the premature baboon model of BPD, which included elastin (ELN), gastrin-releasing polypeptide (GRP), and connective tissue growth factor (CTGF). This approach identified highly conserved transcriptional responses to mechanical ventilation and may facilitate identification of therapeutic targets to reduce the side effects of this valuable treatment.

bronchopulmonary dysplasia; hyperoxia

MECHANICAL VENTILATION is frequently required to maintain oxygenation of neonates in respiratory distress or adults with acute lung injury, such as acute respiratory distress syndrome (ARDS). However, mechanical ventilation can also increase vascular permeability and induce inflammation. Acute lung injury requiring ventilation occurs at an estimated rate of 78.9 per 100,000 adult persons and results in age-dependent in-hospital mortality averaging 38.5% (68). Although mechanical ventilation is often necessary for patients presenting with respiratory distress, it frequently causes additional lung injury (73). Similarly, infants born before 30 wk of gestation, weighing <1,500 g, commonly develop bronchopulmonary dysplasia (BPD), a chronic lung disease characterized by failed morphological development (6), in response to ventilation with supplemental oxygen. BPD is the most common disease of premature infants (29).

Address for reprint requests and other correspondence: R. A. Pierce, Washington Univ. School of Medicine, Campus Box 8052, 660 S. Euclid Ave., St. Louis, MO 63110 (e-mail: rpierce@dom.wustl.edu).

Deleterious effects of mechanical ventilation with supplemental oxygen are supported by findings that both infants and adults with acute lung injury ventilated at lower tidal volumes are at a lower risk for prolonged hospital stay and death (3, 29). In both infants and adults, the side effects of mechanical ventilation with supplemental oxygen are identical to other forms of acute lung injury, including pulmonary edema (10, 82), oxidative stress responses (16, 26), aberrant immune system activation and inflammation (64, 94), and the apoptotic death of lung epithelial cells (22, 54). Synergism between ventilation and sepsis exacerbates inflammation and damage (2). Collectively, injury caused by mechanical ventilation of the lungs is referred to as ventilator-induced lung injury (VILI).

While several rodent and nonhuman primate models of VILI are currently in use in both neonates and adults, it is unclear to what degree they replicate the pathology of the human disease. However, orthologous stress responses that predict outcomes across different species have been identified in response to radiation exposure (28), and there is great interest in identifying conserved genomic responses in cancer (36) and aging (55). The identification of conserved transcriptional profiles in aging, neoplasia, and stress responses suggests that cross-species analysis can improve discriminatory power between physiological states by eliminating unrelated biological noise. Similarly, earlier microarray work in VILI hypothesized that conserved transcriptional responses were more likely to be related to the stimulus (34, 50).

In the present study, we tested a much larger group of 114 whole lung microarray samples in four species and five mouse strains. To reduce false discovery rates (FDRs), we identified and adjusted for a large proportion of unmodeled variation with surrogate variable analysis (SVA) (49) and used updated, sequence-verified "definitions" for Affymetrix microarrays (21). Because computational methods have proven utility in identifying the upstream regulatory mechanisms of disease, we used a computational method to predict the targets of biologically relevant, differentially expressed transcription factors (TFs). Our results provide a basis for potential therapeutic intervention.

METHODS

Baboon model of BPD. The experimental model, which closely duplicates treatments for preterm human infants, has recently been described in detail (60). Animal studies were performed at the Southwest Foundation for Biomedical Research (San Antonio, TX) in accordance with the National Research Council's *Guide for the Care and Use of Laboratory Animals*, and the Animal Care Committee of the Southwest Foundation for Biomedical Research approved all

protocols. Fetal baboons were delivered by hysterotomy at 125 ± 2 days or 140 ± 2 days of gestation (term = 175 days) after the pregnant dams received 6 mg of betamethasone at 48 h and 2 h before delivery. The premature baboons were intubated, treated with surfactant (Survanta at 4 mg/kg), and placed on positive-pressure ventilation with tidal volumes of 4–6 ml/kg to maintain P_{CO_2} of 45–55 mmHg, with supplemental O_2 as needed to maintain arterial P_{O_2} at 40–60 mmHg, for 14 days. Premature baboons delivered at 140 days and killed at delivery served as gestational controls for the ventilated treatment group. Tissue from one animal was hybridized to each Affymetrix HG-U133Av2 microarray. There were no technical replicates or pooling in the microarray study.

Reverse transcription and second strand synthesis. Total RNA was isolated from samples of snap-frozen peripheral lung tissue with a commercial kit (RNAqueous, Ambion). RNA quality and concentration were assessed by Agilent technology (Palo Alto, CA), a capillary electrophoresis-based technique.

First strand synthesis was accomplished by using 10 μg of total RNA plus a "spike" of nonvertebrate mRNAs as internal controls, a poly(dT) primer with a T7 RNA polymerase adaptor, and Invitrogen's SuperScript II reverse transcriptase. *Escherichia coli* DNA polymerase I and RNase H were used for second strand synthesis, and T4 DNA polymerase was used to "polish" the double-stranded product. The cDNA products were then purified with phenol-chloroform extraction and ethanol precipitation.

Amplification and fragmentation of target for gene array hybridizations. A commercial kit (Enzo, Farmingdale, NY) was used to generate high yields of RNA transcripts from the cDNAs that were primed with a T7 adapter oligo(dT) primer. RNA was synthesized with biotin-labeled oligonucleotides and then purified with the RNeasy reagent and protocol from Qiagen (Valencia, CA). After purification, target was fragmented to facilitate hybridization, and quality and concentration were assessed again by Agilent analysis.

Bioinformatic analysis. All analyses were performed with the R statistical package (version 2.7.0) (63) and Bioconductor libraries (version 2.1) (31). Individual analyses and citations therein are described in the following sections.

Annotation of microarray data/identification of orthologs. We downloaded .CSV-formatted annotation data for the Affymetrix HG-U133Av2 human oligonucleotide microarray from the support section of the Affymetrix website (version 25, dated 3/18/08). The ProbeMatchDB database identified cross-species orthologs by UniGene ID (83).

Previously published/publicly available lung microarray data. Supplemental File S1 contains the sources and unique identifiers for all samples used in the present study.[1] Only unpooled, individual biological samples that could be verified as such were used. To preserve the highest possible number of probe sets for statistical testing, certain chip series that were otherwise acceptable were preferentially eliminated because of relatively small numbers of probe sets on that particular chip series, including GSE6044 and GSE2368. Eliminating those two series resulted in an approximately twofold increase in orthologous genes available for testing (data not shown).

Data normalization. The raw data were reannotated with updated CDF definitions, built for UniGene IDs, version 10 (21). Human CDF definitions were used for baboon data. All Affymetrix .CEL files were normalized in R with the RMA algorithm (42). Normalizations were carried out individually for each Affymetrix chip series. Log_2 data from all 114 samples were scaled to mean zero and variance one within each individual sample in order to minimize technical variation before SVA and statistical testing.

Statistical testing of data sets from multiple species. All samples were partitioned into control and ventilated groups, and significant surrogate variables were identified with the SVA method (49) as implemented in the "sva" library, version 1.1.0, for R. These were specified as covariates for the ANOVA. *P* values were converted to FDR-adjusted *q* values by the method of Benjamini and Hochberg (9) as implemented in the "p.adjust" function in R. *q*-Value distributions were compared with the two-sample Kolmogorov-Smirnov (KS) test in R. To compare results with and without the 17 human samples, we used the "cor" and "cor.test" functions in R.

Statistical testing and visualization of baboon groups. After normalization and data preprocessing outlined above, statistical testing was performed separately for the baboon data. The Rank Products algorithm (12) was used from the "RankProd" package (version 2.80) for R. Heat maps were generated with the "heatmap" function in R; dendrograms on heat maps were generated with the "hclust" function in R and complete linkage.

TaqMan quantitative RT-PCR of baboon groups. Quantitative real-time PCR (qRT-PCR) was performed to confirm the key results from the DNA microarray analysis. Identical pooled baboon RNA samples used for microarray were used for qRT-PCR. The following Taqman probes were used: ATF3 (Hs00910173-m1), EREG (Hs00154995-m1), FOS (Hs00170630-m1), GRP (Hs00181852-m1), GAPDH (Hs02758991-g1). Complementary DNA synthesized with SuperScript II reverse transcriptase (Invitrogen) was mixed with Taq Universal Master Mix and TaqMan probe. Relative differences among the samples between control and ventilated baboons were determined with the $\Delta\Delta C_T$ (where C_T is cycle threshold) method. Briefly, a ΔC_T value was calculated for each sample with the C_T values for GAPDH and the target genes. The $\Delta\Delta C_T$ values were then calculated by subtracting the ΔC_T of the control group from the ΔC_T of the ventilated group. The $\Delta\Delta C_T$ values were converted to fold differences versus the control by raising 2 to the power $\Delta\Delta C_T$ ($2^{-\Delta\Delta C_T}$).

Identification of upstream binding motifs. The Promoter Analysis Pipeline (PAP) was used to predict genes with *cis*-regulatory elements bound by selected TFs in human, rat, and mouse (15). For this purpose, we used the Perl API (application programming interface) implementation of this method freely available at **http://bioinformatics.wustl.edu/webTools/PromoterSearch.do** (14).

Detection of significantly altered gene ontologies and transcription factor binding motifs. Using the annotations downloaded from **www.affymetrix.com**, we organized all probe sets' Gene Ontology (GO) (5) annotations into Biological Process (BP), Cellular Component (CC), and Molecular Function (MF) subcategories. For all GO subcategories with at least five genes, the "ks.test" function in R (1-tailed test) was used to test for significant differences in the distributions of *P* values for genes in each GO category. We randomly sampled 10,000 sets of genes for all gene sets' sizes and computed a one-tailed KS test statistic for each draw, e.g., the *P* value of a category with 20 genes was calculated by comparing it with the *P* value distribution of 10,000 KS tests, where each test compared the *P* values of a set of 20 randomly drawn genes to the *P* values of all genes. Then, for each category, *P* values for gene set enrichment were produced by dividing the number of randomly drawn *P* values more significant than the observed *P* value by the number of randomly drawn *P* values (in all cases, 10,000). *P* values were then adjusted for FDR as above.

We downloaded the PAP database (see above) and examined regions predicted to be conserved between human and mouse. For genes shared between our data sets, we associated a position-weight matrix (PWM) from PAP with a gene only if the R score for the PWM (15) was in the top 5% of all PWM R scores for that gene. We used the KS test to identify significant differences in the distributions of *P* values for genes binding a given motif. As for ontology testing, we did not consider sets with fewer than 5 members and calculated *P* values by randomly sampled sets of 10,000 *P* values for each group size, followed by FDR adjustment as above. For high-scoring PWMs displayed in Table 6, if multiple PWMs targeted the same TF, only the most significant result is presented in the table.

[1] Supplemental Material for this article is available online at the Journal website.

RESULTS

Statistical testing of cross-species data set. To identify transcriptional events that were conserved across multiple species in response to mechanical ventilation of the lung, we aggregated all available whole lung Affymetrix oligonucleotide microarray data from public databases (Fig. 1). The final "cross-species" data set included 90 healthy and 24 ventilated samples of various ages, four species, and both sexes (Supplemental File S1). The mouse data included five inbred mouse strains. The probeMatchDB (83) was used to match orthologs from human, baboon, mouse, and rat, yielding 2,531 probe sets available in all samples for statistical testing. Supplemental File S2 contains normalized expression values for the entire data set.

There were large differences between samples owing to batch effects; genetic, species, sex, and age differences; and other unmodeled effects. We used SVA to identify and quantify systematic, confounding variation due to factors orthogonal to experimental design (49). In the cross-species data set, SVA identified four significant surrogate variables, which were included as covariates for statistical testing. Supplemental Figure S1 shows that all probe sets were significantly affected by at least one surrogate variable.

We tested the 2,531 orthologous probe sets for significant expression changes between the 90 control and 24 ventilated samples. *P* values were adjusted for FDR (9), and 60 significant genes at $q < 5E^{-3}$ are presented in Table 1. FDR-adjusted *q* values with and without inclusion of surrogate variables are compared in Fig. 2. Because the cross-species group included only nonventilated human samples (i.e., there were no ventilated humans), we repeated the identical analysis as for the cross-species group, this time omitting those 17 human sam-

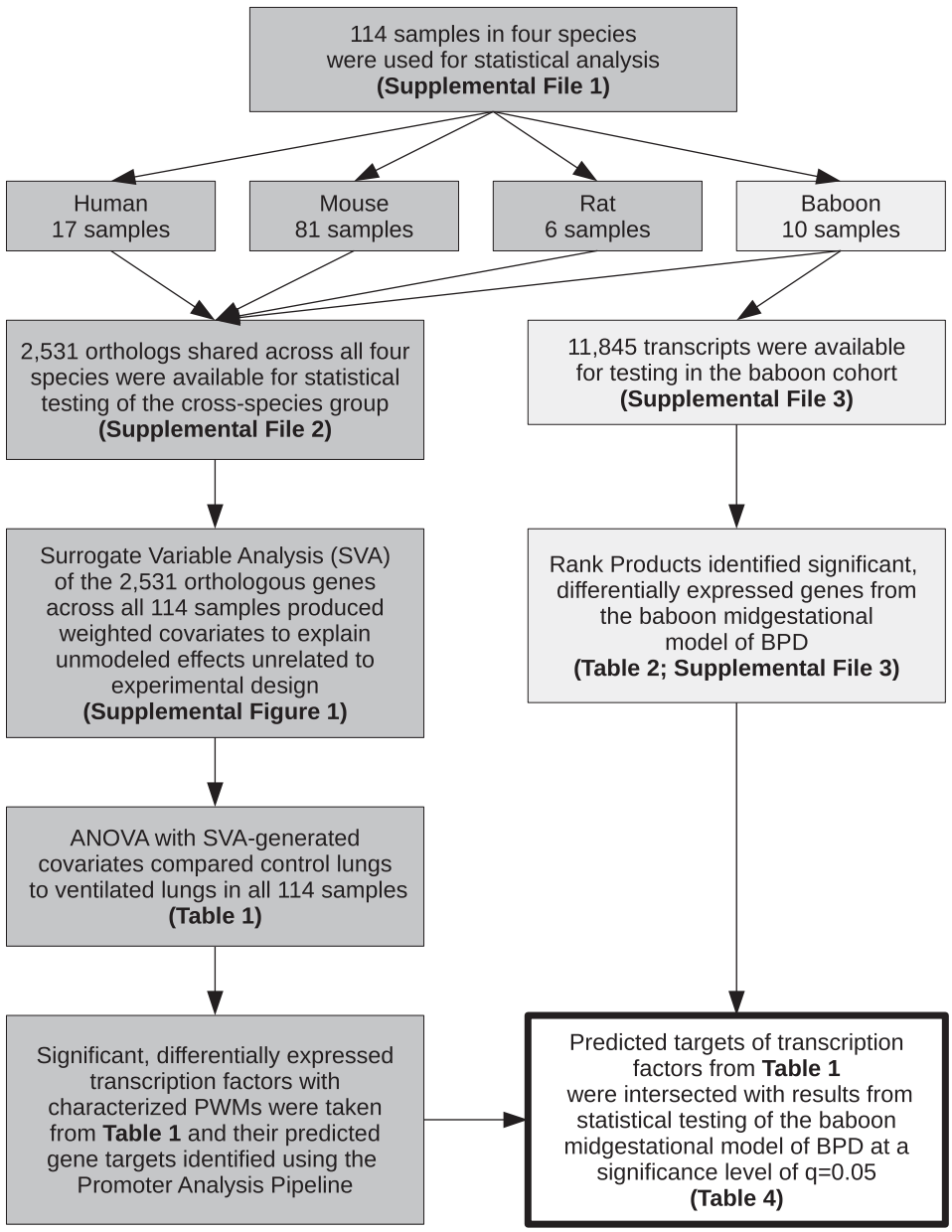

Fig. 1. Analysis overview. Schematic diagram of data sources and analysis procedures. BPD, bronchopulmonary dysplasia; PWM, position-weight matrix.

Table 1. *Significant differentially expressed probe sets from cross-species data set*

UniGene ID	FX	P_{RAW}	P_{SVA}	q_{RAW}	q_{SVA}	Gene Title	Gene Symbol
Hs.25333	1.63	4.94E-03	5.01E-09	1.48E-02	6.35E-06	Interleukin 1 receptor, type II	IL1R2
Hs.79334	1.40	8.41E-02	2.52E-09	1.35E-01	6.35E-06	Nuclear factor, interleukin 3 regulated	NFIL3
Hs.161839	1.58	7.85E-02	1.78E-07	1.28E-01	9.50E-05	Matrix metallopeptidase 8 (neutrophil collagenase)	MMP8
Hs.202453	1.29	1.89E-01	1.39E-07	2.62E-01	9.50E-05	V-myc myelocytomatosis viral oncogene homolog (avian)	MYC
Hs.501890	1.30	1.89E-01	1.88E-07	2.62E-01	9.50E-05	Adenosine monophosphate deaminase (isoform E)	AMPD3
Hs.163484	1.23	2.05E-05	4.76E-07	3.70E-04	1.43E-04	Forkhead box A1	FOXA1
Hs.277035	−1.17	8.75E-01	5.09E-07	9.04E-01	1.43E-04	Monoglyceride lipase	MGLL
Hs.487046	1.24	2.00E-01	4.66E-07	2.74E-01	1.43E-04	Superoxide dismutase 2, mitochondrial	SOD2
Hs.534293	1.41	2.99E-03	4.77E-07	1.02E-02	1.43E-04	Serpin peptidase inhibitor, clade A (α-1 antiproteinase, antitrypsin), member 3	SERPINA3
Hs.460	1.53	6.29E-01	1.10E-06	6.97E-01	2.79E-04	Activating transcription factor 3	ATF3
Hs.459265	1.27	9.61E-01	1.44E-06	9.70E-01	3.03E-04	Interferon-stimulated exonuclease gene 20 kDa	ISG20
Hs.527973	1.43	4.61E-03	1.43E-06	1.39E-02	3.03E-04	Suppressor of cytokine signaling 3	SOCS3
Hs.24485	−1.31	2.24E-01	1.60E-06	3.00E-01	3.12E-04	Structural maintenance of chromosomes 3	SMC3
Hs.86724	1.21	8.83E-01	1.79E-06	9.10E-01	3.23E-04	GTP cyclohydrolase 1	GCH1
Hs.491582	1.31	8.14E-03	2.19E-06	2.18E-02	3.47E-04	Plasminogen activator, tissue	PLAT
Hs.62192	1.37	1.27E-08	2.11E-06	1.60E-05	3.47E-04	Coagulation factor III (thromboplastin, tissue factor)	F3
Hs.108112	−1.16	1.85E-07	3.08E-06	4.51E-05	4.59E-04	Polymerase (DNA directed), ε3 (p17 subunit)	POLE3
Hs.167046	1.26	9.83E-01	4.48E-06	9.85E-01	6.29E-04	Adenosine A2b receptor	ADORA2B
Hs.724	−1.23	1.91E-02	5.35E-06	4.17E-02	7.13E-04	Thyroid hormone receptor, α (erythroblastic leukemia viral (v-erb-a) oncogene homolog, avian)	THRA
Hs.370771	1.31	2.29E-02	5.87E-06	4.82E-02	7.43E-04	Cyclin-dependent kinase inhibitor 1A (p21, Cip1)	CDKN1A
Hs.162877	1.33	3.62E-03	8.46E-06	1.17E-02	1.02E-03	ADP-ribosylation factor GTPase activating protein 3	ARFGAP3
Hs.115263	1.23	4.70E-02	9.82E-06	8.46E-02	1.11E-03	Epiregulin	EREG
Hs.301921	1.24	4.98E-01	1.01E-05	5.79E-01	1.11E-03	Chemokine (C-C motif) receptor 1	CCR1
Hs.247280	−1.15	6.46E-04	1.43E-05	3.40E-03	1.51E-03	RanBP-type and C3HC4-type zinc finger containing 1	RBCK1
Hs.446079	−1.10	3.22E-01	1.60E-05	4.04E-01	1.62E-03	Carboxypeptidase D	CPD
Hs.441047	1.27	2.20E-02	1.74E-05	4.67E-02	1.62E-03	Adrenomedullin	ADM
Hs.592130	−1.22	1.12E-04	1.82E-05	1.05E-03	1.62E-03	Nuclear receptor subfamily 1, group D, member 1	NR1D1
Hs.8867	1.36	5.01E-04	1.69E-05	2.83E-03	1.62E-03	Cysteine-rich, angiogenic inducer, 61	CYR61
Hs.920	1.33	3.28E-01	1.86E-05	4.11E-01	1.62E-03	AT-rich interactive domain 5A (MRF1-like)	ARID5A
Hs.522632	1.41	1.41E-01	1.94E-05	2.05E-01	1.63E-03	TIMP metallopeptidase inhibitor 1	TIMP1
Hs.131226	−1.24	2.61E-01	2.19E-05	3.40E-01	1.79E-03	BCL2/adenovirus E1B 19 kDa interacting protein 3-like	BNIP3L
Hs.25647	1.43	2.71E-03	3.55E-05	9.51E-03	2.68E-03	FBJ murine osteosarcoma viral oncogene homolog	FOS
Hs.371240	1.27	1.99E-07	3.60E-05	4.51E-05	2.68E-03	A kinase (PRKA) anchor protein 12	AKAP12
Hs.527295	−1.15	1.39E-02	3.59E-05	3.25E-02	2.68E-03	Ectonucleotide pyrophosphatase/phosphodiesterase 1	ENPP1
Hs.33446	−1.25	2.79E-01	4.55E-05	3.58E-01	3.20E-03	Nuclear receptor subfamily 5, group A, member 2	NR5A2
Hs.416073	1.46	3.39E-03	4.81E-05	1.13E-02	3.20E-03	S100 calcium binding protein A8	S100A8
Hs.438231	1.17	4.13E-01	4.68E-05	4.98E-01	3.20E-03	Tissue factor pathway inhibitor 2	TFPI2
Hs.551213	−1.32	6.67E-01	4.93E-05	7.32E-01	3.20E-03	Coronin, actin binding protein, 2B	CORO2B
Hs.591767	−1.22	4.43E-01	4.61E-05	5.26E-01	3.20E-03	Centrin, EF-hand protein, 3 (CDC31 homolog, yeast)	CETN3
Hs.534338	1.19	3.22E-06	5.17E-05	1.56E-04	3.27E-03	Protein phosphatase 4 (formerly X), catalytic subunit	PPP4C
Hs.310781	−1.27	2.56E-08	5.36E-05	1.93E-05	3.31E-03	Transcribed locus, strongly similar to NP_035148.1 sequestosome 1	NA
Hs.297413	1.32	1.10E-01	5.50E-05	1.67E-01	3.31E-03	Matrix metallopeptidase 9 (gelatinase B, 92 kDa gelatinase, 92 kDa type IV collagenase)	MMP9
Hs.152536	1.19	1.33E-06	5.87E-05	1.13E-04	3.45E-03	Proteasome (prosome, macropain) 26S subunit, nonATPase, 6	PSMD6
Hs.1420	−1.17	1.25E-02	6.04E-05	3.00E-02	3.47E-03	Fibroblast growth factor receptor 3	FGFR3
Hs.386168	−1.09	7.79E-02	6.63E-05	1.27E-01	3.58E-03	Inositol hexakisphosphate kinase 1	IP6K1
Hs.558364	1.14	5.08E-01	6.65E-05	5.88E-01	3.58E-03	Origin recognition complex, subunit 4-like (yeast)	ORC4L
Hs.613075	1.18	5.00E-02	6.41E-05	8.89E-02	3.58E-03	Diacylglycerol *O*-acyltransferase homolog 1 (mouse)	DGAT1
Hs.135471	1.11	3.35E-02	7.70E-05	6.46E-02	4.06E-03	Neugrin, neurite outgrowth associated	NGRN
Hs.34114	−1.15	8.27E-04	8.17E-05	3.98E-03	4.13E-03	ATPase, Na^+/K^+ transporting, α2 (+) polypeptide	ATP1A2
Hs.75498	1.37	2.51E-05	8.13E-05	4.21E-04	4.13E-03	Chemokine (C-C motif) ligand 20	CCL20
Hs.303090	−1.14	1.07E-02	9.04E-05	2.68E-02	4.48E-03	Protein phosphatase 1, regulatory (inhibitor) subunit 3C	PPP1R3C
Hs.1424	−1.17	1.33E-01	9.88E-05	1.95E-01	4.81E-03	Flavin containing monooxygenase 1	FMO1
Hs.321231	1.20	2.71E-03	1.02E-04	9.51E-03	4.87E-03	UDP-Gal:βGlcNAc β 1,4- galactosyltransferase, polypeptide 3	B4GALT3
Hs.16355	1.18	1.15E-04	1.04E-04	1.08E-03	4.88E-03	Myosin, heavy chain 10, nonmuscle	MYH10
Hs.262858	1.17	1.17E-08	1.12E-04	1.60E-05	4.88E-03	Partner of NOB1 homolog (*S. cerevisiae*)	PNO1
Hs.459940	1.22	1.08E-04	1.14E-04	1.04E-03	4.88E-03	Lipopolysaccharide-induced TNF factor	LITAF
Hs.524134	−1.19	1.44E-03	1.13E-04	5.97E-03	4.88E-03	GATA binding protein 3	GATA3
Hs.567366	−1.25	2.54E-06	1.11E-04	1.49E-04	4.88E-03	Phospholipase A2, group X	PLA2G10
Hs.80132	−1.28	4.21E-01	1.08E-04	5.05E-01	4.88E-03	Sorting nexin 15	SNX15
Hs.89690	1.53	2.72E-01	1.18E-04	3.51E-01	4.99E-03	Chemokine (C-X-C motif) ligand 3	CXCL3

False discovery rate (FDR)-adjusted *P* values from testing the cross-species data set. Sixty significant, differentially expressed transcripts were identified by ANOVA between 90 control whole lung samples and 24 ventilated whole lung samples from multiple species (Supplemental File S1 lists sample details). FX, fold change; q_{RAW}, FDR-adjusted *q* values without inclusion of surrogate variables; q_{SVA}, FDR-adjusted *q* values with inclusion of surrogate variables; P_{RAW}, P_{SVA}, corresponding raw *P* values before FDR adjustment.

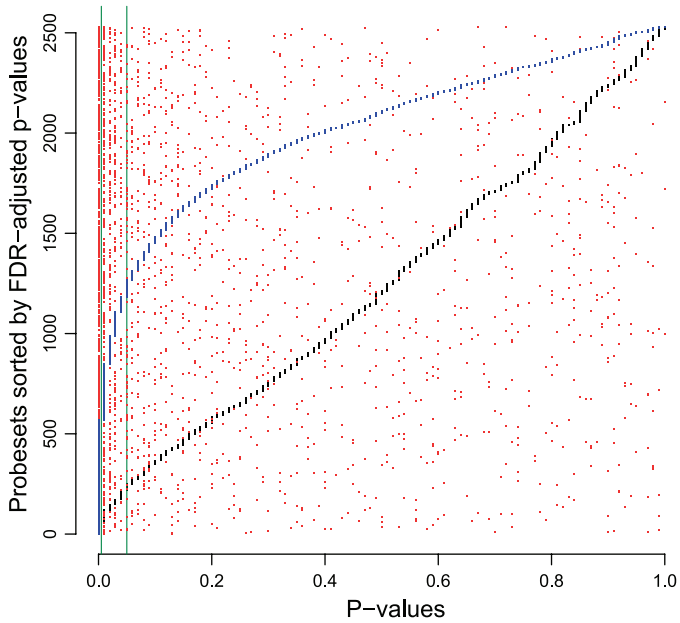

Fig. 2. *P* values from testing the cross-species data set. Sorted, surrogate variable analysis (SVA)-adjusted q values from the entire data set of 2,531 orthologs are plotted in black. Superimposed in red are corresponding q values without SVA adjustment; these q values are overlaid in ascending order in blue. Vertical green lines indicate $q = 0.005$ and $q = 0.05$. q Values without SVA adjustment appear inflated. Both sets of q values were adjusted for false discovery rate (FDR) and were significantly different from one another ($P < 1E^{-15}$; Kolmogorov-Smirnov test).

ples, and compared the resulting q values with those from the entire cross-species group. The correlation between the two sets of q values across the 60 highly significant, differentially expressed transcripts was 0.728, which was highly significant ($P = 4.40E^{-11}$). As expected, given the larger number of statistics, across the entire group of 2,531 transcripts in the cross-species data set, the correlation was higher (0.980) and also highly significant ($P = 2.20E^{-16}$). All 60 differentially expressed genes were still highly significantly differentially expressed when the human samples were omitted; the largest q value when the human group was omitted was $2.33E^{-2}$. Supplemental File S3 contains a direct comparison of the q values with and without human samples.

Statistical testing of baboon groups. We performed another statistical analysis (Fig. 1), using only the baboon cohort, with the nonparametric Rank Products method (12) because of the limited baboon sample size ($n = 10$). Rank Products uses a permuted fold change method to determine significance and generate FDR-adjusted q values. Table 2 contains the most significant, differentially expressed genes at $q < 1E^{-4}$ for which no random permutations produced more extreme statistics. Supplemental File S4 contains additional expression data for all probe sets in the baboon cohort.

Comparison with previously published microarray studies. To directly compare our results from both analyses with those of previously published microarray studies of VILI in smaller sample groups, we examined the set of 37 genes previously aggregated by Wurfel (90) from four existing microarray studies (2, 18, 24, 34). Of the 37 genes highlighted by Wurfel as being significantly differentially expressed in at least two previously published microarray studies, 17 were within the set of 2,531 genes in the cross-species group and 28 were within the baboon group. With a significance level of $q = 0.05$, of the 17 shared with the cross-species group only 8 were deemed significantly differentially expressed by us (Supplemental File S5), and of the 28 shared with the baboon group only 6 were significantly differentially expressed in that group (Supplemental File S6).

qRT-PCR confirmation of selected transcripts. Selected transcripts were chosen on the basis of their statistical significance in the data sets for TaqMan verification using pooled baboon mRNA samples (Table 3). This was done by using identical samples as for microarray. TaqMan fold changes between pooled groups of control and ventilated baboons were in good agreement with microarray data.

Bioinformatic prediction of gene regulatory mechanism. Recent work has shown that small changes in the availability of TFs can have profound effects on gene expression, such as during development of the immune system, where relative concentrations of a single TF determine cell fate (23). The transcriptional response to mechanical ventilation in the cross-species data set was the result of both long- and short-term (i.e., chronic and acute) signaling events, and differentially expressed TFs were likely to have aberrantly regulated downstream target genes.

Previous work has shown that within a given tissue, TFs with functional roles that are highly conserved between rodents and primates can have very species-specific target gene activation (57). Ideally, further analysis of the baboon group would allow for this possibility and use information from the cross-species analysis to prioritize results of testing the baboon group. Of the TFs in Table 1, PWMs are defined for ATF3, FOS, and MYC. Both ATF3 and FOS were significantly differentially expressed also in the baboon data set (ATF3 $q = 6.80E^{-3}$; FOS $q = 5E^{-4}$; Supplemental File S4) and were verified by TaqMan (Table 3). We used PAP (14) to make computational predictions of genes with *cis*-regulatory regions likely to be bound by both ATF3 and FOS (15). Table 4 shows results from PAP that were merged with the list of significant differentially expressed genes from the baboon group at $q = 5E^{-2}$. Although MYC was highly significant in the cross-species data set ($q = 1E^{-4}$) and upregulated ~40% within the baboon group, the change was not significant ($P > 1E^{-1}$) within this group; however, because, like FOS and other AP1 components, MYC is transcribed in response to mechanical stimuli (7, 69), it seemed likely that MYC did not reach significance because of inadequate power in this group of 10 samples. Supplemental File S7 is an analysis identical to that from Table 4, with predicted targets of ATF3, FOS, and MYC in the baboon model. The results were quite similar, with the similarity between gene sets possibly explained by the abundance of MYC binding sites in the mammalian genome. Figure 3 shows overall gene expression levels in the baboon BPD model for the combined set of significant transcripts from Tables 2 and 4.

Detection of significantly altered gene ontologies and transcription factor binding motifs. To get an overview of large-scale changes in gene expression, we examined GO categories for significant overall changes in gene expression and tested whether differentially expressed genes had an overrepresentation of any TF consensus binding sites. While χ^2- or hypergeometric tests are commonly used for this purpose, empirical

Table 2. *Significant differentially expressed probe sets from baboon cohort*

UniGene ID	FX	q_{RP}	Gene Title	Gene Symbol
Hs.154036	7.50	<1.00E-04	Pleckstrin homology-like domain, family A, member 2	PHLDA2
Hs.532634	4.59	<1.00E-04	Interferon, α-inducible protein 27	IFI27
Hs.654444	4.52	<1.00E-04	S100 calcium binding protein A4	S100A4
Hs.591346	4.29	<1.00E-04	Connective tissue growth factor	CTGF
Hs.518448	3.60	<1.00E-04	Lysosomal-associated membrane protein 3	LAMP3
Hs.153444	3.13	<1.00E-04	Gastrin-releasing peptide	GRP
Hs.495728	3.12	<1.00E-04	Pirin (iron-binding nuclear protein)	PIR
Hs.444569	3.11	<1.00E-04	Transmembrane protein 49 /// microRNA 21	MIRN21 /// TMEM49
Hs.654592	2.98	<1.00E-04	Titin	TTN
Hs.201688	2.83	<1.00E-04	Chitinase 1 (chitotriosidase)	CHIT1
Hs.40403	2.75	<1.00E-04	Cbp/p300-interacting transactivator, with Glu/Asp-rich carboxy-terminal domain, 1	CITED1
Hs.365706	2.70	<1.00E-04	Matrix Gla protein	MGP
Hs.696144	2.67	<1.00E-04	NA	NA
Hs.382202	2.67	<1.00E-04	Chitinase 3-like 1 (cartilage glycoprotein-39)	CHI3L1
Hs.406678	2.57	<1.00E-04	Acyl-CoA synthetase long-chain family member 1	ACSL1
Hs.391561	2.49	<1.00E-04	Fatty acid binding protein 4, adipocyte	FABP4
Hs.655491	−2.16	<1.00E-04	Hydroxyprostaglandin dehydrogenase 15-(NAD)	HPGD
Hs.606773	−2.22	<1.00E-04	NA	NA
Hs.36053	−2.23	<1.00E-04	Chromosome 5 open reading frame 13	C5orf13
Hs.29802	−2.24	<1.00E-04	Slit homolog 2	SLIT2
Hs.289795	−2.27	<1.00E-04	Metallophosphoesterase domain containing 2	MPPED2
Hs.13245	−2.31	<1.00E-04	Plasticity-related gene 1	LPPR4
Hs.654434	−2.39	<1.00E-04	Angiotensin I-converting enzyme (peptidyl-dipeptidase A) 1	ACE
Hs.696099	−2.46	<1.00E-04	NA	NA
Hs.591908	−2.72	<1.00E-04	A kinase (PRKA) anchor protein 2 /// PALM2-AKAP2	AKAP2 /// PALM2-AKAP2
Hs.17109	−3.29	<1.00E-04	Integral membrane protein 2A	ITM2A
Hs.522666	−3.39	<1.00E-04	Aminolevulinate, δ-, synthase 2 (sideroblastic/hypochromic anemia)	ALAS2
Hs.644183	−3.80	<1.00E-04	NA	NA
Hs.655195	−4.21	<1.00E-04	Hemoglobin, ε1	HBE1
Hs.483444	−6.98	<1.00E-04	Chemokine (C-X-C motif) ligand 14	CXCL14
Hs.25647	2.13	5.00E-04	v-fos FBJ murine osteosarcoma viral oncogene homolog	FOS
Hs.460	1.67	6.80E-03	Activating transcription factor 3	ATF3
Hs.202453	1.42	1.25E-01	v-myc myelocytomatosis viral oncogene homolog (avian)	MYC

Thirty significant, differentially expressed transcripts ($q < 1E^{-4}$) were identified with the Rank Products algorithm (12) when the baboon group was tested separately. q values are estimated at $<1E^{-4}$ because none of the randomly drawn fold changes from the permuted data set was more extreme. q_{RP}, FDR-adjusted q values. For comparison, and because they were also highly significant, FOS, ATF3, and MYC are also shown. NA, gene assignment not available or unknown.

distribution-free (EDF) tests do not require an arbitrary significance cutoff and have more power to detect distributional changes (8). To identify significantly altered GO categories with at least five members represented in either the cross-species data set or the baboon data set, we used the KS test and corrected for FDR. Table 5 shows the 10 most significant categories for each of the 2 comparisons in each category and their corresponding FDR.

In addition to our focused analysis of putative ATF3 and FOS targets, it was also of great interest to do a broad search for other TFs likely to be preferentially activated by ventilation. Six hundred thirty-six characterized PWMs from TRANSFAC (87) and JASPAR (70) are included in the PAP database. After filtering to associate each gene with only the highest-scoring PWMs (METHODS), we used the KS test to predict TFs that were most likely to have driven differential gene expression. Table 6 shows the 10 most significant PWMs after FDR correction.

InterPro domains were also tested for overrepresentation, but very few domains reached even marginal significance in either comparison. Complete results for GO categories, PWMs, and InterPro domains are contained in Supplemental File S8.

Table 3. *Microarray and TaqMan fold changes for baboon data set*

Transcript	Microarray FX	TaqMan FX
ATF3	1.67 ± 0.22	5.54
EREG	3.30 ± 1.26	2.55
FOS	2.14 ± 1.17	2.60
GRP	3.13 ± 0.63	3.86

Selected transcripts were verified in pooled baboon samples with TaqMan analysis using GAPDH as internal control. Standard error of fold change calculated according to Jacobs and Dinman (43).

DISCUSSION

Cross-species identification of transcriptional targets of mechanical ventilation. Using microarrays, we identified previously unknown modulators of VILI in the lung by aggregating data from divergent genetic backgrounds, species, and ages to generate estimates of gene expression changes that were likely to be highly conserved. The quality of our results was greatly improved by two steps—SVA (49) and updated definitions (21).

The combination of different microarray chip versions and the matching of orthologs reduced the number of available probe sets for statistical testing by a factor of more than four compared with the baboon cohort. This also reduced the multiple testing burden and allowed a large increase in sample size. The 2,531 probe sets interrogated more well-annotated genes with known orthologs in both primates and rodents, but

Table 4. *Predicted targets of ATF3 and FOS that were significantly differentially expressed in preterm baboon model of BPD*

Probe Set	FX	q_{RP}	Rank Percentile	Gene Title	Gene Symbol
Hs.75969	−1.45	4.00E-02	0.07	Proline-rich nuclear receptor coactivator 1	PNRC1
Hs.443577	1.73	3.00E-03	0.09	Tumor necrosis factor receptor superfamily, member 21	TNFRSF21
Hs.153444	3.13	<1.00E-04	0.33	Gastrin-releasing peptide	GRP
Hs.514795	−1.55	1.20E-02	0.43	Nucleolar protein 4	NOL4
Hs.388927	−1.47	3.00E-02	0.51	YY1 transcription factor	YY1
Hs.591346	4.29	<1.00E-04	0.75	Connective tissue growth factor	CTGF
Hs.644108	−1.54	1.10E-02	0.86	Glypican 3	GPC3
Hs.647061	1.53	2.30E-02	0.91	Elastin (supravalvular aortic stenosis, Williams-Beuren syndrome)	ELN
Hs.355899	1.79	6.00E-03	1.02	Tumor necrosis factor receptor superfamily, member 12A	TNFRSF12A
Hs.527078	−1.40	4.50E-02	1.08	Peroxisome proliferator-activated receptor, γ, coactivator 1, α	PPARGC1A
Hs.474751	1.43	4.10E-02	1.35	Myosin, heavy polypeptide 9, nonmuscle	MYH9
Hs.478588	1.52	1.90E-02	1.70	B-cell CLL/lymphoma 6 (zinc finger protein 51)	BCL6
Hs.435001	−1.55	6.00E-03	1.81	Kruppel-like factor 10	KLF10
Hs.155097	−1.82	1.00E-03	2.04	Carbonic anhydrase II	CA2
Hs.377783	−1.49	1.90E-02	2.29	Adenylate cyclase activating polypeptide 1 (pituitary) receptor type I	ADCYAP1R1
Hs.436792	−1.44	3.70E-02	2.43	LIM domain only 4	LMO4
Hs.530930	−1.74	1.00E-03	2.69	Zinc finger protein 423	ZNF423
Hs.9701	−1.40	4.60E-02	2.77	Growth arrest and DNA-damage-inducible, γ	GADD45G
Hs.82002	−1.45	3.60E-02	2.81	Endothelin receptor type B	EDNRB
Hs.551213	−1.55	1.20E-02	3.08	Coronin, actin binding protein, 2B	CORO2B
Hs.512690	1.46	3.10E-02	3.73	Surfactant, pulmonary-associated protein B	SFTPB
Hs.476273	−1.61	1.10E-02	4.24	Calcium channel, voltage-dependent, α2/δ subunit 2	CACNA2D2
Hs.198072	−1.60	1.10E-02	4.51	Phosphodiesterase 4B, cAMP-specific (phosphodiesterase E4 dunce homolog, *Drosophila*)	PDE4B
Hs.409223	1.54	1.20E-02	4.65	Signal sequence receptor, δ (translocon-associated protein δ)	SSR4
Hs.75812	1.58	1.00E-02	4.96	Phosphoenolpyruvate carboxykinase 2 (mitochondrial)	PCK2

BPD, bronchopulmonary dysplasia; FX, fold change calculated only from the 10 baboon samples; q_{RP}, Rank Products q value for significance of differential expression between control and ventilated baboon samples; Rank Percentile, percentile rank of likelihood of ATF3 and FOS regulation (e.g., ELN has a Rank Percentile of 0.91, meaning that ELN ranks in the top 0.91% of all 9,834 genes in the PAP database for the likelihood of being regulated by ATF3 and FOS).

it is unlikely that the use of only the 2,531 orthologs introduced additional bias in represented ontologies or genome coverage.

Combining divergent microarray samples appeared to identify physiologically relevant and highly conserved responses but also introduced substantial noise that might have obscured our results, shown by comparison of q value distributions. Statistical testing of microarray data is typically confounded by unmodeled covariates (49), and combining data from different laboratories, experiments, and species increased the amount of confounding noise. SVA is useful because it identifies so-called "surrogate variables" and converts them into weighted covariates for adjustment in statistical testing. Our results suggest that SVA is a reasonable alternative to nonparametric tests. While there is little purpose in identifying the confounding effects, as they lack predictive power or diagnostic value, our results do suggest that previous microarray studies of VILI that have combined array data from different species have had high FDRs, and that careful reanalysis of public data sets not included here is likely to be fruitful. Indeed, comparison of our results with those aggregated by Wurfel (90) across multiple, previously published studies supports this.

Because they affected all transcripts, the covariates likely represented a mixture of technical and biological effects. Technical effects certainly included batch effects from differences in laboratory protocols, varied hybridization efficiencies, and scanning artifacts. Although we did not systematically identify the sources of variation, biological effects may have been greater and more elusive. Complex biological systems exhibit large transcriptional fluctuations of many genes. For example, the circadian cycle affects airway inflammation in asthma (53) and affects many genes in health, depending on tissue (61). A likely source of biological noise was the immune system. The healthy lung has a resident immune population, and the ventilated lung undergoes an inflammatory immune response. In healthy subjects, studies of immune gene expression are confounded by many factors related to previous immune system activation, diet, and stress (40).

Previous work showed that there are many annotation errors with the 25mer oligonucleotide sequences on Affymetrix chips; many do not bind any known sequence, and many bind nonspecifically to multiple transcripts, producing FDRs of 30–40% with standard analysis procedures (21). We addressed this problem by using updated, more accurate definitions for the Affymetrix probe sets. While qRT-PCR can technically validate positives, it does not resolve insufficient sample sizes or confounding effects.

There are several obvious biases of our study that arose from the zealous use of public data in order to boost sample size. Each set of experiments used in the cross-species data set was performed in a separate lab and was limited to a single species; therefore, species and batch are confounded. For many of the data sets obtained from the NCBI Gene Expression Omnibus (GEO), age and sex information were not provided. In the cross-species data set, mice were overrepresented and there were no ventilated human samples. However, the mice were heterogeneous; five common, inbred mouse strains were represented in the control group and two were in the ventilated group. Combining different mouse strains in microarray experiments can reduce noise and identify conserved responses (39). Because previous work has shown great variability in lung responses to hyperoxia between inbred laboratory mouse strains (84), we believe that the approach of combining these data from different strains, with SVA, further reduced noise. The C57BL/6J strain, which was the majority of ventilated

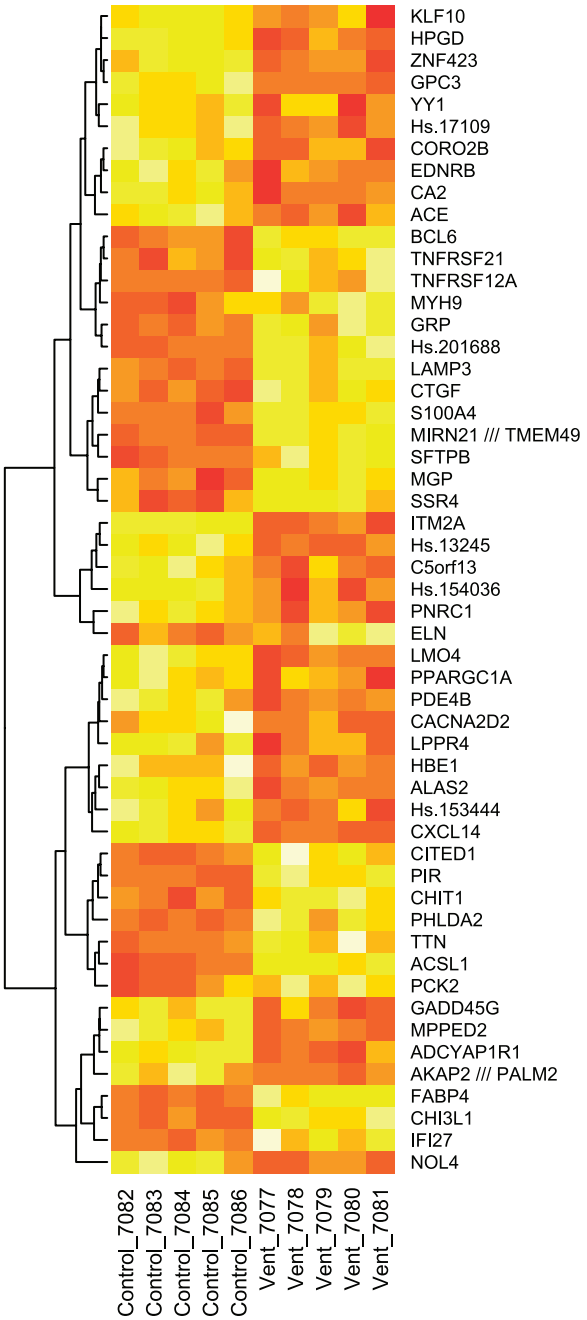

Fig. 3. Heat map of differential gene expression in the baboon model of BPD. Expression values of 62 transcripts from Table 2 and Table 4 (both tables from the baboon cohort) were clustered by hierarchical clustering with complete linkage. Sample clustering is omitted, as the probe sets in this figure were chosen on the basis of their ability to discriminate between control and ventilated samples. Lighter yellow indicates upregulation; darker red indicates downregulation.

mouse samples (13 of 16 total), is a median representative of lung damage in hyperoxia (84) and was unlikely to introduce large bias to the ventilated group. Within the cross-species data set, the overall proportion of primates among normal control and ventilated samples is quite similar—approximately 24% of control samples and 21% of ventilated samples were either human or baboon, while the intraprimate balance was less ideal. However, given the existing batch effects and missing covariate information from the public rodent data, obtaining a larger sample size was our foremost priority. To identify the most conserved responses, we deliberately chose, at the outset, to increase sample size in lieu of using a completely balanced study design, and comparison of our results from the cross-species data set to the repeat analysis minus human samples indicated that the net result was a loss of power rather than a species-specific bias. Despite the drawbacks, our results suggest that incorporation of publicly available data from divergent species can improve results, particularly in complicated and expensive disease models where samples are necessarily limited, such as the baboon midgestational model of BPD.

Highly conserved transcriptional responses. Many differentially expressed genes from the cross-species analysis have not been previously associated with VILI, while others do have established roles in oxidative stress, mechanotransduction, and pulmonary disease, helping validate this approach. Among differentially expressed genes, MMP8 inhibits alveolo-capillary protein leakage in ventilated mice (25) and is required for polymorphonuclear neutrophil chemotaxis in response to LPS-induced inflammatory response (77). AMPD3 decreases inosine monophosphate levels, recruiting neutrophils to the reperfused lung (62). SOCS3 is a well-known inflammatory gene whose adenoviral expression in rodent lung causes increased lung vascular permeability (30). LITAF (LPS-induced TNF-α factor) is a TF whose activation by p38α, in response to LPS, binds STAT6B and activates TNF-α (75, 76). TNF levels are predictive of severity of ARDS (37), and TNFRp55-null mice are protected from pulmonary edema by high tidal volume (86). The A2B receptor is a well-studied proinflammatory gene that induces various cytokines, including MCP1 (80), and is increased in the lung by mechanical ventilation (27). The biological relevance of significant differentially expressed genes obtained by our analysis suggests improvement over previous analyses of divergent lung ventilation data.

Regulatory pathway prediction. ATF3 and FOS likely regulate other genes in the context of the mechanical strain, immune activation, and hyperoxia of VILI, as both TFs are themselves transcriptionally regulated, early/adaptive stress-response genes. Because both bind AP1 sites (1), we hypothesized that they act coordinately to modulate transcription of clinically relevant genes in VILI. Because the concentration of TFs is tightly regulated in living cells (65), likely because of potent effects of changes in their availability (e.g., Ref. 23), small changes likely produce substantial downstream effects, particularly for factors such as FOS with widespread binding sites. Indeed, previous studies have established the presence of AP1 components in VILI, as FOS is an early response gene in the ventilated lung (79), and increased AP1 binding occurs preferentially with mechanical ventilation compared with LPS treatment (2, 32). FOS is also induced by diverse mechanical stimuli and oxidative stress (4, 38, 41) and has prominent roles in immune activation in lung alveoli (35). Similarly, ATF3 protects against oxidative damage (93), attenuates inflammation by repressing CCL4 release from macrophages (46), and has been proposed to be a key modulator of macrophage activation (65). Because selective inhibition of neutrophil influx, despite hyperoxia, in the neonatal rat model of BPD protects against lung damage (92), it is likely that much of the pulmonary damage in BPD is due to the massive infiltration of immune cells, which release various ECM remodeling en-

Table 5. *Results of gene set enrichment testing*

Cross Species				Baboon			
Category Title	Category Size	P_{KS}	q_{KS}	Category Title	Category Size	P_{KS}	q_{KS}
Gene Ontology Biological Process							
Cell fate determination	5	5.00E-04	1.72E-01	RNA splicing	142	<3.00E-04	<4.79E-02
cAMP biosynthetic process	5	6.00E-04	1.72E-01	Protein amino acid phosphorylation	426	<3.00E-04	<4.79E-02
Regulation of blood pressure	25	1.40E-03	2.22E-01	mRNA processing	168	3.00E-04	4.79E-02
Platelet-derived growth factor receptor signaling pathway	6	2.10E-03	2.22E-01	ATP synthesis-coupled proton transport	23	1.20E-03	9.58E-02
Inflammatory response	73	2.80E-03	2.22E-01	Transforming growth factor-β receptor signaling pathway	27	1.20E-03	9.58E-02
Transcription	242	2.90E-03	2.22E-01	Negative regulation of cell proliferation	155	1.20E-03	9.58E-02
Behavioral fear response	5	3.10E-03	2.22E-01	Response to stress	112	1.70E-03	1.14E-01
Transcription from RNA polymerase II promoter	42	3.10E-03	2.22E-01	Cell proliferation	238	1.90E-03	1.14E-01
Positive regulation of smooth muscle cell proliferation	11	4.80E-03	2.71E-01	Organ morphogenesis	107	2.40E-03	1.18E-01
Regulation of transcription	91	4.80E-03	2.71E-01	Respiratory gaseous exchange	18	3.00E-03	1.18E-01
Gene Ontology Cellular Component							
Neuromuscular junction	10	2.45E-02	9.95E-01	Lysosomal membrane	41	<1.00E-04	<4.60E-03
Nuclear speck	7	2.67E-02	9.95E-01	Cytoplasm	2,461	<1.00E-04	<4.60E-03
Microtubule	30	3.19E-02	9.95E-01	Spliceosome	85	1.00E-04	4.60E-03
Kinetochore	9	4.55E-02	9.95E-01	Lysosome	136	2.00E-04	7.00E-03
Cell surface	51	5.54E-02	9.95E-01	Nuclear chromosome, telomeric region	5	1.20E-03	3.34E-02
Cytoplasmic vesicle	45	5.70E-02	9.95E-01	Hemoglobin complex	6	2.40E-03	5.56E-02
Cortical actin cytoskeleton	5	7.62E-02	9.95E-01	Proteinaceous extracellular matrix	214	3.60E-03	7.15E-02
Spliceosome	12	8.50E-02	9.95E-01	Ruffle	31	5.50E-03	9.56E-02
Heterotrimeric G protein complex	6	8.88E-02	9.95E-01	Proton-transporting two-sector ATPase complex	28	1.42E-02	1.97E-01
Nicotinic acetylcholine-gated receptor-channel complex	6	9.94E-02	9.95E-01	Integrin complex	24	1.47E-02	1.97E-01
Gene Ontology Molecular Function							
3′,5′-Cyclic nucleotide phosphodiesterase activity	7	2.00E-03	5.76E-01	Protein binding	4,047	<6.00E-04	<4.53E-02
DNA binding	251	6.30E-03	6.62E-01	Protein kinase inhibitor activity	19	6.00E-04	4.53E-02
Platelet-derived growth factor receptor binding	5	9.10E-03	6.62E-01	Protein kinase activity	401	7.00E-04	4.53E-02
Transcription factor activity	151	9.20E-03	6.62E-01	Nucleotide binding	1,226	7.00E-04	4.53E-02
Sequence-specific DNA binding	86	1.26E-02	7.26E-01	Peptidyl-prolyl *cis-trans* isomerase activity	23	8.00E-04	4.53E-02
Transcription regulator activity	57	1.58E-02	7.58E-01	RNA binding	400	1.70E-03	8.02E-02
Microtubule motor activity	8	2.08E-02	7.63E-01	Calcium-dependent protein binding	10	2.00E-03	8.09E-02
Protease binding	6	2.12E-02	7.63E-01	Cholesterol binding	12	3.80E-03	1.34E-01
Phosphoinositide phospholipase C activity	10	2.95E-02	9.35E-01	Cytochrome-b_5 reductase activity	5	4.70E-03	1.36E-01
Phospholipase C activity	7	3.80E-02	9.35E-01	Endopeptidase inhibitor activity	65	5.10E-03	1.36E-01

category title, Gene Ontology (GO) category name; category size, total number of probe sets in the data set assigned to the given GO category or predicted to have regulatory regions bound by a given transcription factor (TF); P_{KS}, unadjusted P value; q_{KS}, FDR-adjusted q value; consensus site, corresponding bound TF. Note that statistics were determined by 10,000 random draws in all cases; statistics reported as "less than (<)" resulted from no random draws being more significant than observed for the given gene set.

zymes, including elastase (13). Mice null for ATF3 show an increased immune response in a model of airway inflammation (33), indicating a likely role for ATF3 in modulating the immune response during ventilation. Because, of the TFs identified from the cross-species data set as being significantly differentially expressed PWMs were only available for ATF3, FOS, and MYC, there was certainly an inherent bias introduced, because we could not identify targets of the remaining TFs. Identification of consensus sites and generation of PWMs for the remaining TFs identified in the cross-species data set would allow finer dissection of the transcriptional regulatory mechanisms in VILI, which underscores the need for identification of PWMs for the remaining TFs.

Midgestational baboon model of BPD. Currently, there are only a very small number of reports of human oligonucleotide microarrays paired with baboon tissue (19, 20, 48, 71), and there are not yet high-quality genome sequence data available for the baboon with which to validate probe sets. However, the baboon midgestational model replicates human BPD, the most severe manifestation of VILI, with high fidelity (17), and our microarray analysis of this model has revealed compelling targets for further study. More transcripts were available for testing the baboon cohort separately because not all orthologs are known in the four species or were not queried on all platforms. However, given the gross inaccuracies of the original annotations for Affymetrix GeneChips (21) as discussed

Table 6. *Results of testing PWM enrichment*

Position-Weight Matrixes							
Cross Species				Baboon			
Consensus Site (PWM)	Category Size	P_{KS}	q_{KS}	Consensus Site (PWM)	Category Size	P_{KS}	q_{KS}
myogenin/NF-1	42	2.00E-03	6.38E-01	cEBP	178	<1.00E-04	<5.70E-03
Nkx	30	3.40E-03	6.38E-01	AREB6	180	<1.00E-04	<5.70E-03
STAT5A	50	4.30E-03	6.38E-01	COMP1	181	<1.00E-04	<5.70E-03
TBX5	44	4.90E-03	6.38E-01	YY1	185	<1.00E-04	<5.70E-03
Retroviral poly(A) signal	35	7.20E-03	6.38E-01	c-Ets-1(p54)	194	<1.00E-04	<5.70E-03
E2F	42	7.20E-03	6.38E-01	SRF	197	<1.00E-04	<5.70E-03
VDR	45	7.20E-03	6.38E-01	Egr-3	101	1.00E-04	5.70E-03
E2F	45	9.90E-03	7.37E-01	MEF-2	186	1.00E-04	5.70E-03
E2F-4:DP-1	39	1.07E-02	7.37E-01	c-Ets-1(p54)	190	1.00E-04	5.70E-03
E2F	46	1.24E-02	7.69E-01	SPI-B	197	1.00E-04	5.70E-03

Position-weight matrix (PWM) enrichment was done as for GO contained in the cross-species and baboon groups being bound by a particular TF (METHODS).

above and the extremely high coding sequence conservation overall between baboon and human, we believe the species differences are marginal compared with the artifacts that would arise from using any unverified sequence definitions for any primate. However, because the smaller sample size of the baboon group and species-mismatched hybridizations might lead to false discoveries, we used TaqMan qRT-PCR to first verify selected, key results, followed by computational prediction of ATF3-FOS targets to prioritize the results of testing the baboon cohort separately. This also permitted identification of (evolutionarily divergent) transcriptional targets of ATF3-FOS that may be unique to primates; previous work has shown that TFs with highly conserved roles can have very divergent binding sites between mouse and human tissues (57).

Age-related transcriptional differences likely explain much of the variation in our results when the baboon cohort was tested separately from the entire cross-species data set, as the baboons were the only gestational samples in this study. This also likely contributed to the lower overlap between the set of 37 genes prioritized by Wurfel (90) and the results of testing the baboon group compared with the overlap between those 37 genes and the results of testing the cross-species group. In addition, necessarily higher FDRs in the baboon group, due to the smaller sample size, may also have contributed to lower overlap. The smaller percentage of differentially expressed genes from the cross-species analysis was likely relevant to all ages and species. Our results from the baboon cohort suggest that there are unique components of the transcriptional response to mechanical ventilation during development and that additional studies are required to precisely identify the age-dependent mechanisms that appear to confer varied susceptibility to VILI.

Our analysis suggests key roles for ATF3 and FOS in regulating the immune response associated with mechanical ventilation during the development of BPD. Among ATF3-FOS targets in the baboon model were genes known to be dysregulated in chronic lung injury in premature neonates, where mechanical ventilation and supplemental oxygen are primary risk factors (44). Our results support established roles for transforming growth factor-β (TGF-β) signaling in VILI and identified previously unknown modulators. The 27 genes of the "TGF-β receptor signaling pathway" Biological Process ontology were associated with lung ventilation at a 10% FDR (baboon group, Table 5). TGF-β and ATF3 can cooperate in transducing injury signals in epithelium (45), and TGF-β can also drive epithelial to mesenchymal transition, which is involved in the pathogenesis of fibrotic disorders of the lung (85). Similarly, several ATF3-FOS target genes identified in this study are known targets of TGF-β signaling, including ELN, GPC3, CTGF, and GRP. ELN, which provides important structural properties to the lung, is upregulated by mechanical ventilation in premature neonatal lambs (59), baboons (56, 59), and mice (11). ELN is normally expressed in the lung during development and is quiescent in healthy adult lung (52), but aberrant ELN expression is induced in fibrotic disorders of the lung (72), in pulmonary hypertension (78), and during lung growth in response to pneumonectomy (47). GPC3, which has not been previously associated with VILI, was repressed in our samples and is repressed by TGF-β (66). CTGF was upregulated in our study and is induced by high tidal ventilation in newborn rats (89). GRP was significantly upregulated in the baboon data set and contributes to impaired lung development in premature baboons with mechanical ventilation support (74). These predicted target genes support the hypothesis that ATF3 and FOS interact to regulate genes involved in the pathogenesis of neonatal injury from mechanical ventilation.

Other genes from the baboon model included those with previous roles that merit further study in VILI. Most compelling are TNFRSF21, which has known roles in eosinophil accumulation and airway inflammation (81); ADCYAP1R1 [mice null for this gene have pulmonary hypertension and die of heart failure soon after birth (58)]; and TNFRSF12A, a receptor for the TNF family cytokine TWEAK, which modulates inflammation and apoptosis (88). In human bronchial epithelial cells, the induction of inflammatory markers by TWEAK requires TNFRSF12A (91).

Detection of significantly altered gene ontologies and motifs. Previous work has suggested that EDF tests can outperform the hypergeometric alternatives in the detection of broad changes in gene expression across entire classes of genes (8). They allow discovery of relevant, coordinate groups of genes by examining the entire distribution of statistics. Our results are consistent with previous work suggesting important roles for inflammation, stress response, and the aberrant reactivation of developmental pathways in VILI. Various ontologies related to binding were associated with the response to ventilation, likely due to an elevated stress response as well as oxidative damage to DNA and proteins (51, 67). However, our results for GO and

TF consensus motif testing consistently had a substantially higher FDR in the cross-species data set compared with the baboon group. This is likely due to the combination of fairly high numbers of categories (in both groups) with at least five genes, adding to the multiple testing burden, as well as the smaller overall size of all categories represented in the cross-species data set (data not shown). Methodology for the analysis of gene set enrichment is currently an area of active research.

For motif detection, PAP was chosen because it contains PWMs from TRANSFAC and JASPAR that are predicted to be in highly conserved regions. Our results from the analysis provide more important regulatory clues in VILI and suggest roles for other factors. These results and others suggest that experimental manipulation of these predicted, conserved upstream regulatory mechanisms is likely to reveal the events that shape outcomes of patients undergoing ventilation with supplemental oxygen.

Conclusion. Our results reveal a highly conserved response to mechanical ventilation of the lung and have shown that ATF3 and FOS are differentially expressed across several animal models of VILI, where a pronounced immune response has been directly linked to pulmonary damage. We identified genes regulated by ATF3 and AP1 as candidates for targeted intervention to reduce complications from mechanical ventilation. Because recent work suggests prominent roles for ATF3 in the regulation of airway inflammation (33), treatments that induce ATF3 in the neonatal or adult lung before ventilation and supplemental oxygen may be protective by reducing the massive immune response that contributes to pulmonary ECM remodeling and damage. This suggests that by dissecting the transcriptional response based on regulatory predictions, specific components can be targeted in order to improve outcomes in patients. Identification of the binding sites for many other TFs that were differentially expressed will allow further dissection of the upstream signaling pathways modulated by mechanical ventilation. Future studies in neonatal and adult knockout mice undergoing mechanical ventilation will allow for finer genetic dissection of regulatory mechanisms activated during ventilation.

ACKNOWLEDGMENTS

David Beebe, Gary Stormo, and John Witte read the manuscript and participated in helpful discussions. Li-Wei Chang helped with the PAP analysis. Sina Gharib shared raw data from GEO series GSE2411. Manhong Dai provided flat file copies of the ProbeMatchDB. We appreciate the helpful comments provided by Bruce Aronow.

Present address of K. S. Kompass: Dept. of Epidemiology and Biostatistics and Institute for Human Genetics, University of California, San Francisco, CA 94158.

GRANTS

This work was supported by National Institutes of Health (NIH) Grant 5U01-HL-063387-06. K. S. Kompass was supported by awards to the Department of Ophthalmology and Visual Sciences at Washington University from a Research to Prevent Blindness, Inc. Unrestricted grant; NIH Vision Core Grant P30-EY-02687; NEI Research Training Program in the Vision Sciences Grant 5-T32-EY-13360; and NIH Grant R25-CA-112355.

DISCLOSURES

No conflicts of interest, financial or otherwise, are declared by the author(s).

K. S. Kompass and R. A. Pierce designed the study and wrote the paper. K. S. Kompass did the analysis. G. Deslee performed qRT-PCR studies. C. Moore handled tissue specimens and isolated RNA for array experiments. D. McCurnin supervised all animal studies.

REFERENCES

1. **Allan AL, Albanese C, Pestell RG, LaMarre J.** Activating transcription factor 3 induces DNA synthesis and expression of cyclin D1 in hepatocytes. *J Biol Chem* 276: 27272–27280, 2001.
2. **Altemeier WA, Matute-Bello G, Frevert CW, Kawata Y, Kajikawa O, Martin TR, Glenny RW.** Mechanical ventilation with moderate tidal volumes synergistically increases lung cytokine response to systemic endotoxin. *Am J Physiol Lung Cell Mol Physiol* 287: L533–L542, 2004.
3. **Amato MB, Barbas CS, Medeiros DM.** Effect of a protective-ventilation strategy on mortality in the acute respiratory distress syndrome. *N Engl J Med* 338: 347–354, 1998.
4. **Amstad PA, Krupitza G, Cerutti PA.** Mechanism of c-fos induction by active oxygen. *Cancer Res* 52: 3952–3960, 1992.
5. **Ashburner M, Ball CA, Blake JA, Botstein D, Butler H, Cherry JM, Davis AP, Dolinski K, Dwight SS, Eppig JT.** Gene Ontology: tool for the unification of biology. *Nat Genet* 25: 25–29, 2000.
6. **Baraldi E, Filippone M.** Chronic lung disease after premature birth. *N Engl J Med* 357: 1946–1955, 2007.
7. **Bauters C, Moalic JM, Bercovici J, Mouas C, Emanoil-Ravier R, Schiaffino S, Swynghedauw B.** Coronary flow as a determinant of c-myc and c-fos proto-oncogene expression in an isolated adult rat heart. *J Mol Cell Cardiol* 20: 97–101, 1988.
8. **Ben-Shaul Y, Bergman H, Soreq H.** Identifying subtle interrelated changes in functional gene categories using continuous measures of gene expression. *Bioinformatics* 21: 1129–1137, 2004.
9. **Benjamini Y, Hochberg Y.** Controlling the false discovery rate: a practical and powerful approach to multiple testing. *J R Stat Soc Ser B* 57: 289–300, 1995.
10. **Bland RD.** Neonatal chronic lung disease in the post-surfactant era. *Biol Neonate* 88: 181–191, 2005.
11. **Bland RD, Ertsey R, Mokres LM, Xu L, Jacobson BE, Jiang S, Alvira CM, Rabinovitch M, Shinwell ES, Dixit A.** Mechanical ventilation uncouples synthesis and assembly of elastin and increases apoptosis in lungs of newborn mice. Prelude to defective alveolar septation during lung development? *Am J Physiol Lung Cell Mol Physiol* 294: L3–L14, 2008.
12. **Breitling R, Armengaud P, Amtmann A, Herzyk P.** Rank products: a simple, yet powerful, new method to detect differentially regulated genes in replicated microarray experiments. *FEBS Lett* 573: 83–92, 2004.
13. **Campbell EJ.** Preventive therapy of emphysema. Lessons from the elastase model. *Am Rev Respir Dis* 134: 435–437, 1986.
14. **Chang LW, Fontaine BR, Stormo GD, Nagarajan R.** PAP: a comprehensive workbench for mammalian transcriptional regulatory sequence analysis. *Nucleic Acids Res* 35: W238–W244, 2007.
15. **Chang LW, Nagarajan R, Magee JA, Milbrandt J, Stormo GD.** A systematic model to predict transcriptional regulatory mechanisms based on overrepresentation of transcription factor binding profiles. *Genome Res* 16: 405–413, 2006.
16. **Chang LYL, Subramaniam M, Yoder BA, Day BJ, Ellison MC, Sunday ME, Crapo JD.** A catalytic antioxidant attenuates alveolar structural remodeling in bronchopulmonary dysplasia. *Am J Respir Crit Care Med* 167: 57–64, 2003.
17. **Coalson JJ, Winter VT, Gerstmann DR, Idell S, King RJ, Delemos RA.** Pathophysiologic, morphometric, and biochemical studies of the premature baboon with bronchopulmonary dysplasia. *Am Rev Respir Dis* 145: 872–881, 1992.
18. **Copland IB, Kavanagh BP, Engelberts D, McKerlie C, Belik J, Post M.** Early changes in lung gene expression due to high tidal volume. *Am J Respir Crit Care Med* 168: 1051–1059, 2003.
19. **Cox LA, Nijland MJ, Gilbert JS, Schlabritz-Loutsevitch NE, Hubbard GB, McDonald TJ, Shade RE, Nathanielsz PW.** Effect of 30 per cent maternal nutrient restriction from 0.16 to 0.5 gestation on fetal baboon kidney gene expression. *J Physiol* 572: 67–85, 2006.
20. **Cox LA, Schlabritz-Loutsevitch N, Hubbard GB, Nijland MJ, McDonald TJ, Nathanielsz PW.** Gene expression profile differences in left and right liver lobes from mid-gestation fetal baboons: a cautionary tale. *J Physiol* 572: 59–66, 2006.
21. **Dai M, Wang P, Boyd AD, Kostov G, Athey B, Jones EG, Bunney WE, Myers RM, Speed TP, Akil H.** Evolving gene/transcript definitions significantly alter the interpretation of GeneChip data. *Nucleic Acids Res* 33: e175, 2005.
22. **De Paepe ME, Mao Q, Chao Y, Powell JL, Rubin LP, Sharma S.** Hyperoxia-induced apoptosis and Fas/FasL expression in lung epithelial cells. *Am J Physiol Lung Cell Mol Physiol* 289: L647–L659, 2005.

23. **DeKoter RP, Singh H.** Regulation of B lymphocyte and macrophage development by graded expression of PU.1. *Science* 288: 1439–1441, 2000.
24. **Dolinay T, Kaminski N, Felgendreher M, Kim HP, Reynolds P, Watkins SC, Karp D, Uhlig S, Choi AMK.** Gene expression profiling of target genes in ventilator-induced lung injury. *Physiol Genomics* 26: 68–75, 2006.
25. **Dolinay T, Wu W, Kaminski N, Ifedigbo E, Kaynar AM, Szilasi M, Watkins SC, Ryter SW, Hoetzel A, Choi AMK.** Mitogen-activated protein kinases regulate susceptibility to ventilator-induced lung injury. *PLoS ONE* 3: e1601, 2008.
26. **Dos Santos CC.** Hyperoxic acute lung injury and ventilator-induced/associated lung injury: new insights into intracellular signaling pathways. *Crit Care* 11: 126, 2007.
27. **Douillet CD, Robinson WR III, Zarzaur BL, Lazarowski ER, Boucher RC, Rich PB.** Mechanical ventilation alters airway nucleotides and purinoceptors in lung and extrapulmonary organs. *Am J Respir Cell Mol Biol* 32: 52–58, 2005.
28. **Dressman HK, Muramoto GG, Chao NJ, Meadows S, Marshall D, Ginsburg GS, Nevins JR, Chute JP.** Gene expression signatures that predict radiation exposure in mice and humans. *PLoS Med* 4: e106, 2007.
29. **Eichenwald EC, Stark AR.** Management and outcomes of very low birth weight. *N Engl J Med* 358: 1700–1711, 2008.
30. **Gao H, Hoesel LM, Guo RF, Rancilio NJ, Sarma JV, Ward PA.** Adenoviral-mediated overexpression of SOCS3 enhances IgG immune complex-induced acute lung injury. *J Immunol* 177: 612–620, 2006.
31. **Gentleman RC, Carey VJ, Bates DM, Bolstad B, Dettling M, Dudoit S, Ellis B, Gautier L, Ge Y, Gentry J, Hornik K, Hothorn T, Huber W, Iacus S, Irizarry R, Leisch F, Li C, Maechler M, Rossini AJ, Sawitzki G, Smith C, Smyth G, Tierney L, Yang JY, Zhang J.** Bioconductor: open software development for computational biology and bioinformatics. *Genome Biol* 5: R80, 2004.
32. **Gharib SA, Liles WC, Klaff LS, Altemeier WA.** Noninjurious mechanical ventilation activates a proinflammatory transcriptional program in the lung. *Physiol Genomics* 37: 239–248, 2009.
33. **Gilchrist M, Henderson WR Jr, Clark AE, Simmons RM, Ye X, Smith KD, Aderem A.** Activating transcription factor 3 is a negative regulator of allergic pulmonary inflammation. *J Exp Med* 205: 2349–2357, 2008.
34. **Grigoryev DN, Ma SF, Irizarry RA, Ye SQ, Quackenbush J, Garcia JG.** Orthologous gene-expression profiling in multi-species models: search for candidate genes. *Genome Biol* 5: R34, 2004.
35. **Gwinn MR, Vallyathan V.** Respiratory burst: role in signal transduction in alveolar macrophages. *J Toxicol Environ Health* 9: 27–39, 2006.
36. **Hackett CS, Hodgson JG, Law ME, Fridlyand J, Osoegawa K, de Jong PJ, Nowak NJ, Pinkel D, Albertson DG, Jain A.** Genome-wide array CGH analysis of murine neuroblastoma reveals distinct genomic aberrations which parallel those in human tumors. *Cancer Res* 63: 5266–5273, 2003.
37. **Halbertsma FJ, Vaneker M, Scheffer GJ, van der Hoeven JG.** Cytokines and biotrauma in ventilator-induced lung injury: a critical review of the literature. *Neth J Med* 63: 382–392, 2005.
38. **Hsieh HJ, Cheng CC, Wu ST, Chiu JJ, Wung BS, Wang DL.** Increase of reactive oxygen species (ROS) in endothelial cells by shear flow and involvement of ROS in shear-induced c-fos expression. *J Cell Physiol* 175: 156–162, 1998.
39. **Hwang D, Lee IY, Yoo H, Gehlenborg N, Cho JH, Petritis B, Baxter D, Pitstick R, Young R, Spicer D.** A systems approach to prion disease. *Mol Syst Biol* 5: 252, 2009.
40. **Idaghdour Y, Storey JD, Jadallah SJ, Gibson G.** A genome-wide gene expression signature of environmental geography in leukocytes of Moroccan Amazighs. *PLoS Genet* 4: e1000052, 2008.
41. **Iqbal J, Zaidi M.** Molecular regulation of mechanotransduction. *Biochem Biophys Res Commun* 328: 751–755, 2005.
42. **Irizarry RA, Hobbs B, Collin F, Beazer-Barclay YD, Antonellis KJ, Scherf U, Speed TP.** Exploration, normalization, and summaries of high density oligonucleotide array probe level data. *Biostatistics* 4: 249–264, 2003.
43. **Jacobs JL, Dinman JD.** Systematic analysis of bicistronic reporter assay data. *Nucleic Acids Res* 32: e160, 2004.
44. **Jobe AH, Ikegami M.** Prevention of bronchopulmonary dysplasia. *Curr Opin Pediatr* 13: 124–129, 2001.
45. **Kang Y, Chen CR, Massague J.** A self-enabling TGFbeta response coupled to stress signaling: Smad engages stress response factor ATF3 for Id1 repression in epithelial cells. *Mol Cell* 11: 915–926, 2003.
46. **Khuu CH, Barrozo RM, Hai T, Weinstein SL.** Activating transcription factor 3 (ATF3) represses the expression of CCL4 in murine macrophages. *Mol Immunol* 44: 1609–1616, 2007.
47. **Koh DW, Roby JD, Starcher B, Senior RM, Pierce RA.** Postpneumonectomy lung growth: a model of reinitiation of tropoelastin and type I collagen production in a normal pattern in adult rat lung. *Am J Respir Cell Mol Biol* 15: 611–623, 1996.
48. **Kothapalli KSD, Anthony JC, Pan BS, Hsieh AT, Nathanielsz PW, Brenna JT.** Differential cerebral cortex transcriptomes of baboon neonates consuming moderate and high docosahexaenoic acid formulas. *PLoS ONE* 2: e370, 2007.
49. **Leek JT, Storey JD.** Capturing heterogeneity in gene expression studies by surrogate variable analysis. *PLoS Genet* 3: e161, 2007.
50. **Ma SF, Grigoryev DN, Taylor AD, Nonas S, Sammani S, Ye SQ, Garcia JGN.** Bioinformatic identification of novel early stress response genes in rodent models of lung injury. *Am J Physiol Lung Cell Mol Physiol* 289: L468–L477, 2005.
51. **Maniscalco WM, Watkins RH, Roper JM, Staversky R, O'Reilly MA.** Hyperoxic ventilated premature baboons have increased p53, oxidant DNA damage and decreased VEGF expression. *Pediatr Res* 58: 549–556, 2005.
52. **Mariani TJ, Sandefur S, Pierce RA.** Elastin in lung development. *Exp Lung Res* 23: 131–145, 1997.
53. **Martin RJ.** Location of airway inflammation in asthma and the relationship to circadian change in lung function. *Chronobiol Int* 16: 623–630, 1999.
54. **Martin TR, Hagimoto N, Nakamura M, Matute-Bello G.** Apoptosis and epithelial injury in the lungs. *Proc Am Thorac Soc* 2: 214–220, 2005.
55. **McCarroll SA, Murphy CT, Zou S, Pletcher SD, Chin CS, Jan YN, Kenyon C, Bargmann CI, Li H.** Comparing genomic expression patterns across species identifies shared transcriptional profile in aging. *Nat Genet* 36: 197–204, 2004.
56. **McCurnin DC, Pierce RA, Chang LY, Gibson LL, Osborne-Lawrence S, Yoder BA, Kerecman JD, Albertine KH, Winter VT, Coalson JJ, Crapo JD, Grubb PH, Shaul PW.** Inhaled NO improves early pulmonary function and modifies lung growth and elastin deposition in a baboon model of neonatal chronic lung disease. *Am J Physiol Lung Cell Mol Physiol* 288: L450–L459, 2005.
57. **Odom DT, Dowell RD, Jacobsen ES, Gordon W, Danford TW, MacIsaac KD, Rolfe PA, Conboy CM, Gifford DK, Fraenkel E.** Tissue-specific transcriptional regulation has diverged significantly between human and mouse. *Nat Genet* 39: 730–732, 2007.
58. **Otto C, Hein L, Brede M, Jahns R, Engelhardt S, Grone HJ, Schutz G.** Pulmonary hypertension and right heart failure in pituitary adenylate cyclase-activating polypeptide type I receptor-deficient mice. *Circulation* 110: 3245–3251, 2004.
59. **Pierce RA, Albertine KH, Starcher BC, Bohnsack JF, Carlton DP, Bland RD.** Chronic lung injury in preterm lambs: disordered pulmonary elastin deposition. *Am J Physiol Lung Cell Mol Physiol* 272: L452–L460, 1997.
60. **Pierce RA, Joyce B, Officer S, Heintz C, Moore C, McCurnin D, Johnston C, Maniscalco W.** Retinoids increase lung elastin expression but fail to alter morphology or angiogenesis genes in premature ventilated baboons. *Pediatr Res* 61: 703–709, 2007.
61. **Ptitsyn AA, Zvonic S, Gimble JM.** Digital signal processing reveals circadian baseline oscillation in majority of mammalian genes. *PLoS Comput Biol* 3: e120, 2007.
62. **Qiu FH, Wada K, Stahl GL, Serhan CN.** IMP and AMP deaminase in reperfusion injury down-regulates neutrophil recruitment. *Proc Natl Acad Sci USA* 97: 4267–4272, 2000.
63. **R Foundation for Statistical Computing.** *R: A Language and Environment for Statistical Computing*. Vienna, Austria: R Foundation for Statistical Computing, 2007.
64. **Ranieri VM, Suter PM, Tortorella C, De Tullio R, Dayer JM, Brienza A, Bruno F, Slutsky AS.** Effect of mechanical ventilation on inflammatory mediators in patients with acute respiratory distress syndrome: a randomized controlled trial. *JAMA* 282: 54–61, 1999.
65. **Roach JC, Smith KD, Strobe KL, Nissen SM, Haudenschild CD, Zhou D, Vasicek TJ, Held GA, Stolovitzky GA, Hood LE.** Transcription factor expression in lipopolysaccharide-activated peripheral-blood-derived mononuclear cells. *Proc Natl Acad Sci USA* 104: 16245–16250, 2007.
66. **Romaris M, Bassols A, David G.** Effect of transforming growth factor-beta1 and basic fibroblast growth factor on the expression of cell surface

proteoglycans in human lung fibroblasts. Enhanced glycanation and fibronectin-binding of CD44 proteoglycan, and down-regulation of glypican. *Biochem J* 310: 73–81, 1995.
67. **Rotta AT, Gunnarsson B, Hernan LJ, Fuhrman BP, Steinhorn DM.** Partial liquid ventilation with perflubron attenuates in vivo oxidative damage to proteins and lipids. *Crit Care Med* 28: 202–208, 2000.
68. **Rubenfeld GD, Caldwell E, Peabody E, Weaver J, Martin DP, Neff M, Stern EJ, Hudson LD.** Incidence and outcomes of acute lung injury. *N Engl J Med* 353: 1685–1693, 2005.
69. **Sadoshima J, Jahn L, Takahashi T, Kulik TJ, Izumo S.** Molecular characterization of the stretch-induced adaptation of cultured cardiac cells. An in vitro model of load-induced cardiac hypertrophy. *J Biol Chem* 267: 10551–10560, 1992.
70. **Sandelin A, Alkema W, Engstrom P, Wasserman WW, Lenhard B.** JASPAR: an open-access database for eukaryotic transcription factor binding profiles. *Nucleic Acids Res* 32: D91–D94, 2004.
71. **Seth D, Leo MA, McGuinness PH, Lieber CS, Brennan Y, Williams R, Wang XM, McCaughan GW, Gorrell MD, Haber PS.** Gene expression profiling of alcoholic liver disease in the baboon (*Papio hamadryas*) and human liver. *Am J Pathol* 163: 2303–2317, 2003.
72. **Shifren A, Woods JC, Rosenbluth DB, Officer S, Cooper JD, Pierce RA.** Upregulation of elastin expression in constrictive bronchiolitis obliterans. *Int J Chron Obstruct Pulmon Dis* 2: 593–598, 2007.
73. **Slutsky AS.** Lung injury caused by mechanical ventilation. *Chest* 116: 9S–15S, 1999.
74. **Subramaniam M, Steiner C, Twowmey A, Andreeva S, Yoder BA, Chang LY, Crapo JD, Pierce RA, Cuttitta F, Sunday ME.** Bombesin-like peptides modulate alveolarization and angiogenesis in bronchopulmonary dysplasia. *Am J Respir Crit Care Med* 176: 902–912, 2007.
75. **Tang X, Marciano DL, Leeman SE, Amar S.** LPS induces the interaction of a transcription factor, LPS-induced TNF-alpha factor, and STAT6(B) with effects on multiple cytokines. *Proc Natl Acad Sci USA* 102: 5132–5137, 2005.
76. **Tang X, Metzger D, Leeman S, Amar S.** LPS-induced TNF-alpha factor (LITAF)-deficient mice express reduced LPS-induced cytokine: evidence for LITAF-dependent LPS signaling pathways. *Proc Natl Acad Sci USA* 103: 13777–13782, 2006.
77. **Tester AM, Cox JH, Connor AR, Starr AE, Dean RA, Puente XS, López-Otín C, Overall CM.** LPS responsiveness and neutrophil chemotaxis in vivo require PMN MMP-8 activity. *PLoS ONE* 2: e312, 2007.
78. **Todorovich-Hunter L, Johnson DJ, Ranger P, Keeley FW, Rabinovitch M.** Altered elastin and collagen synthesis associated with progressive pulmonary hypertension induced by monocrotaline. A biochemical and ultrastructural study. *Lab Invest* 58: 184–195, 1988.
79. **Tremblay L, Valenza F, Ribeiro SP, Li J, Slutsky AS.** Injurious ventilatory strategies increase cytokines and c-fos m-RNA expression in an isolated rat lung model. *J Clin Invest* 99: 944–952, 1997.
80. **Vass G, Horvath I.** Adenosine and adenosine receptors in the pathomechanism and treatment of respiratory diseases. *Curr Med Chem* 15: 917–922, 2008.
81. **Venkataraman C, Justen K, Zhao J, Galbreath E, Na S.** Death receptor-6 regulates the development of pulmonary eosinophilia and airway inflammation in a mouse model of asthma. *Immunol Lett* 106: 42–47, 2006.
82. **Verbrugge SJ, Lachmann B, Kesecioglu J.** Lung protective ventilatory strategies in acute lung injury and acute respiratory distress syndrome: from experimental findings to clinical application. *Clin Physiol Funct Imaging* 27: 67–90, 2007.
83. **Wang P, Ding F, Chiang H, Thompson RC, Watson SJ, Meng F.** ProbeMatchDB—a web database for finding equivalent probes across microarray platforms and species. *Bioinformatics* 18: 488–489, 2002.
84. **Whitehead GS, Burch LH, Berman KG, Piantadosi CA, Schwartz DA.** Genetic basis of murine responses to hyperoxia-induced lung injury. *Immunogenetics* 58: 793–804, 2006.
85. **Willis BC, Borok Z.** TGF-beta-induced EMT: mechanisms and implications for fibrotic lung disease. *Am J Physiol Lung Cell Mol Physiol* 293: L525–L534, 2007.
86. **Wilson MR, Goddard ME, O'Dea KP, Choudhury S, Takata M.** Differential roles of p55 and p75 tumor necrosis factor receptors on stretch-induced pulmonary edema in mice. *Am J Physiol Lung Cell Mol Physiol* 293: L60–L68, 2007.
87. **Wingender E, Dietze P, Karas H, Knuppel R.** TRANSFAC: a database on transcription factors and their DNA binding sites. *Nucleic Acids Res* 24: 238–241, 1996.
88. **Winkles JA.** The TWEAK-Fn14 cytokine-receptor axis: discovery, biology and therapeutic targeting. *Nat Rev Drug Discov* 7: 411–425, 2008.
89. **Wu S, Capasso L, Lessa A, Peng J, Kasisomayajula K, Rodriguez M, Suguihara C, Bancalari E.** High tidal volume ventilation activates Smad2 and upregulates expression of connective tissue growth factor in newborn rat lung. *Pediatr Res* 63: 245–250, 2008.
90. **Wurfel MM.** Microarray-based analysis of ventilator-induced lung injury. *Proc Am Thorac Soc* 4: 77–84, 2007.
91. **Xu H, Okamoto A, Ichikawa J, Ando T, Tasaka K, Masuyama K, Ogawa H, Yagita H, Okumura K, Nakao A.** TWEAK/Fn14 interaction stimulates human bronchial epithelial cells to produce IL-8 and GM-CSF. *Biochem Biophys Res Commun* 318: 422–427, 2004.
92. **Yi M, Jankov RP, Belcastro R, Humes D, Copland I, Shek S, Sweezey NB, Post M, Albertine KH, Auten RL.** Opposing effects of 60% oxygen and neutrophil influx on alveologenesis in the neonatal rat. *Am J Respir Crit Care Med* 170: 1188–1196, 2004.
93. **Yoshida T, Sugiura H, Mitobe M, Tsuchiya K, Shirota S, Nishimura S, Shiohira S, Ito H, Nobori K, Gullans SR.** ATF3 protects against renal ischemia-reperfusion injury. *J Am Soc Nephrol* 19: 217–224, 2008.
94. **Zimmerman JJ.** Bronchoalveolar inflammatory pathophysiology of bronchopulmonary dysplasia. *Clin Perinatol* 22: 429–456, 1995.